Available online at www.sciencedirect.com

ScienceDirect

Procedia Engineering 194 (2017) 96 – 103

Procedia Engineering

www.elsevier.com/locate/procedia

10th International Conference on Marine Technology, MARTEC 2016

Computation of Flow Field around Ship Hull including Self Propulsion Characteristics at Varying Rudder Positions

Md. Mashud Karim[a,*], Nabila Naz[a]

[a]*Department of Naval Architecture and Marine Engineering, Bangladesh University of Engineering and Technology, Dhaka-1000, Bangladesh*

Abstract

Flow field around different modern benchmark ship hull with self propulsion characteristics at varying longitudinal positions of rudder is computed using Computation Fluid Dynamics (CFD) technique. Numerical study is performed around bare hull first to determine free surface wave elevation and resistance components. Zonal approach is applied to incorporate 'potential flow solver' in the region outside the boundary layer & wake, 'boundary layer solver' in thin boundary layer region near the hull and 'Navier Stokes solver' in the wake region successively. Lifting Line method coupled with RANS solver is used to compute propeller open and self propulsion characteristics at different positions of rudder. Verification and validation studies for resistance coefficients have also been carried out using ITTC recommended procedure. The present computational method reveals that CFD results of flow field around ship hull with propeller and rudder effects are prospective and can be successfully applied in maritime industry.

Peer-review under responsibility of the organizing committee of the 10th International Conference on Marine Technology.
Keywords: Zonal approach; self propulsion; lifting line model; wake fraction; verification & validation

1. Introduction

Computation of flow field around ship hull including propeller and rudder with changing positions of rudder is very important with growing demands for high efficiency propulsion systems. The propeller open water test has been successfully simulated by various computational methods such as vortex lattice method or boundary element method. However, the simulation of self-propulsion test has not been fully established yet due to the difficulty of calculating the effective wake. The effective wake resulted from the interaction between propeller and ship hull has been studied by many naval hydrodynamic researchers.

Self propulsion characteristics of rotating propeller can be determined with a hierarchy of CFD methods by sliding grid or overset technique. The first computation of this kind was performed for the KCS containership by Löbke [1], though it was not a truly self-propulsion case since both the propeller rps and ship speed were imposed. New approach of coupling a potential flow propeller solver with a CFD solver is being used by Hino [**?**], Kim et al. [3], Tahara et al. [4] and Choi et al. [5]. Recently, Huiping et al. [6] developed a non-interactive body force propeller model allowing computation of propeller rotational speed and the thrust coefficient intended for quick computations.

In the present paper, Shipflow CFD code is used to compute the flow around the ship hull, propeller and rudder. Lifting line method which is coupled with RANS solver is used to compute the propeller characteristics at varying longitudinal rudder positions and compared to each other in order to determine the optimum position of rudder.

* Corresponding author. Tel.:+8801715313384
E-mail address: mashudbuet@gmail.com

Peer-review under responsibility of the organizing committee of the 10th International Conference on Marine Technology.
doi:10.1016/j.proeng.2017.08.122

Nomenclature

Φ	velocity potential
C_w	wave making resistance coefficient
C_v	viscous resistance coefficient
C_t	total resistance coefficient
$\bar{\sigma_{ji}}$	Average stress vector
F_i	body force
R_{ji}	Reynolds stress
F_n	Froude number

2. Computational method

The coordinate system (x, y, z) is defined as origin is located in the undisturbed free surface at fore perpendicular (F.P) of the hull so that the undisturbed incident flow with a constant speed U appears to be a streaming in the positive-x direction with y axis extends to the starboard side and z- axis upwards as shown in Fig. 1(a).

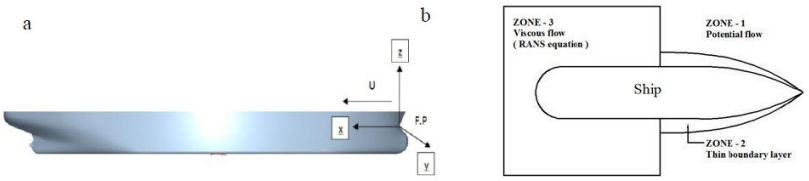

Fig. 1: (a) Cartesian coordinate system; (b) Shipflow zonal approach

To compute the flow around a ship in an efficient way, zonal approach is used as shown in Fig. 1(b). which divides the flow around a ship into three different zones with different solution methods. Region outside the boundary layer and wake is considered to be incompressible, inviscid and irrotational. Therefore, in the outer flow (zone 1), the potential flow theory is employed. The inner flow is divided into the thin boundary layer (zone 2) and stern/wake region (zone 3).

2.1. Governing equation

To determine free-surface shape and the flow far away the hull, panel method solver is used. It is assumed that the fluid is incompressible and inviscid and the flow is irrotational. Consequently, the continuity equation becomes:

$$\vec{\nabla}.\vec{V} = \vec{\nabla}.(\vec{\nabla}\Phi) = \nabla^2\Phi = 0 \tag{1}$$

At the free-surface the kinematic and dynamic boundary conditions have to be imposed. Radiation boundary condition is also necessary to impose so that no waves upstream of the hull shall be created. The viscous flow at stern region is solved with viscous solver using steady RANS equations coupled with the time-averaged continuity equation:

$$\frac{\partial}{\partial x_j}(\bar{u_i}\bar{u_j}) = -\frac{1}{\rho}\frac{\partial p}{\partial x_i} + F_i + \frac{1}{\rho}\frac{\partial}{\partial x_j}(\bar{\sigma_{ji}} + R_{ji})\frac{\partial u_i}{\partial x_i} = 0 \tag{2}$$

2.2. Propeller characteristics

Propeller is modelled by a lifting line method. In this method a propeller with finite number of blade is modelled with a vortex system including hub vortex, bound vortex and helical free vortex.

Typical propeller characteristics are advance coefficient J, thrust coefficient K_t and torque coefficient K_q. The definitions of the parameters are following:

$$J = \frac{V_A}{nD} \quad K_t = \frac{T}{\rho n^2 D^4} \quad K_q = \frac{Q}{\rho n^2 D^5} \tag{3}$$

The generated power P_D by engine is delivered to the propeller and defined by:

$$P_D = 2\pi n Q_n \tag{4}$$

where V_A is advance velocity, T is thrust and Q_n is the generated torque and D is the propeller diameter.

2.3. Boundary conditions and grid generation for viscous flow computation

Boundary types employed are no slip, slip, inflow, and outflow. Both Dirichlet and Neumann boundary conditions are formulated in terms of pressure, velocity , turbulent kinetic energy, and turbulent frequency. Hull geometry is represented by a single block structured grid of H-O type. Additional grids for the propeller and the rudder is fitted with hull by Chimera or overset grid approach.

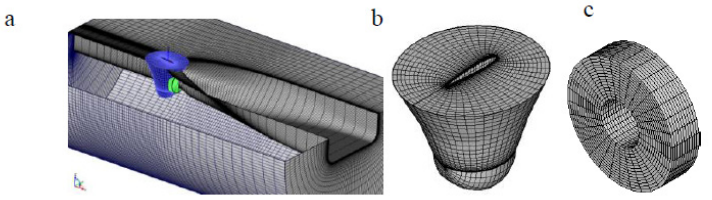

Fig. 2: Grid generation (a) Hull, propeller disc, rudder together; (b) rudder; (c) propeller disc

3. Description of hull, propeller and rudder

3.1. Description of hull

Two modern benchmark ship hull namely KCS (Kriso Container Ship) and JBC (Japan Bulk Carrier) shown in Fig.3, are used for CFD validation. The principal particulars in full and model scale are described in Table 1.

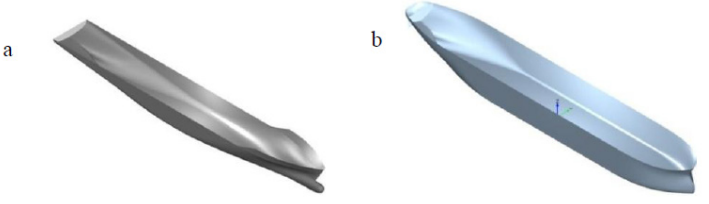

Fig. 3: (a) KCS hull; (b) JBC hull

3.2. Description of propeller and rudder

Propellers models used are KP 505 and DTMB 4119 propellers for KCS and JBC hull respectively. Semi balanced horn rudder is used to analyze the effect of varying rudder positions as shown in Fig.4.

Table 1: Principal particulars for KCS and JBC hull

Hull type	**KCS**		**JBC**	
Main particulars	**Full scale**	**Model scale**	**Full scale**	**Model scale**
Length between perpendiculars (m)	230.0	7.279	280.0	7.0
Maximum beam of waterline (m)	32.2	1.0190	45.0	0.561
Depth (m)	19.0	0.6019	25.0	0.630
Draft (m)	10.8	0.342	16.5	0.423
Block coefficient (CB)	0.651	0.651	0.859	0.858

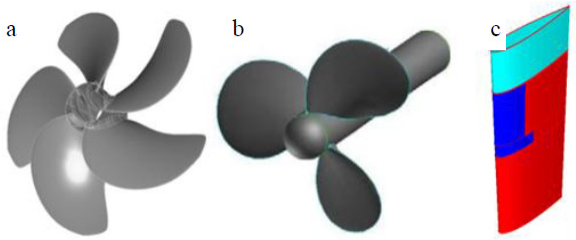

Fig. 4: (a) KP 505; (b) DTMB 4119 propeller; (c) Semi balanced horn rudder

4. Results and discussions

The free-surface wave pattern, wave elevation along the hull, verification and validation of resistance coefficients, propeller open water and self propulsion characteristics at varying rudder positions for both hull are determined in the present work, which are discussed in this section.

4.1. Wave pattern

Computed wave pattern around KCS and JBC hull at Fn. 0.26 with measured results [7] are shown in Fig.5.

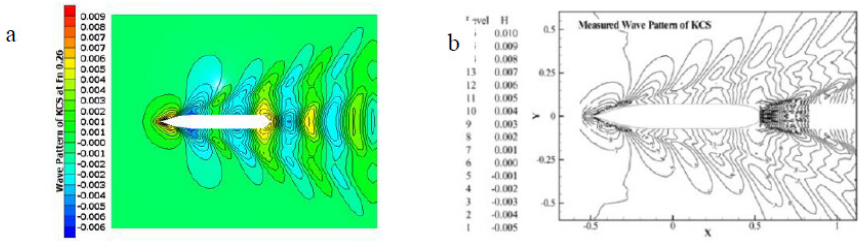

Fig. 5: Wave pattern around KCS hull at Fn.0.26 (a) Computed from Shipflow; (b) Measured result

Computed wave pattern around JBC hull portside is compared with the experimental wave pattern [8] of starboard side at Fn. 0.142 as shown in Fig.6. Both hull consist of a number of transverse and divergent waves. Transverse waves are predominant for KCS hull due to higher Fn. whereas, lower Fn. produce more divergent waves as for the case of JBC here.

4.2. Free-surface wave profile

The computed free-surface wave elevations around KCS and JBC hulls at Fr. 0.26 and at Fr. 0.142 respectively show good agreement with the experimental results [7], [8] as shown in Fig. 7.

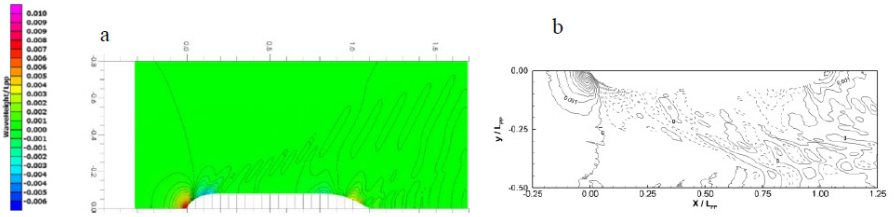

Fig. 6: Wave pattern around JBC hull at Fn.0.142 (a) Computed from Shipflow; (b) Measured result

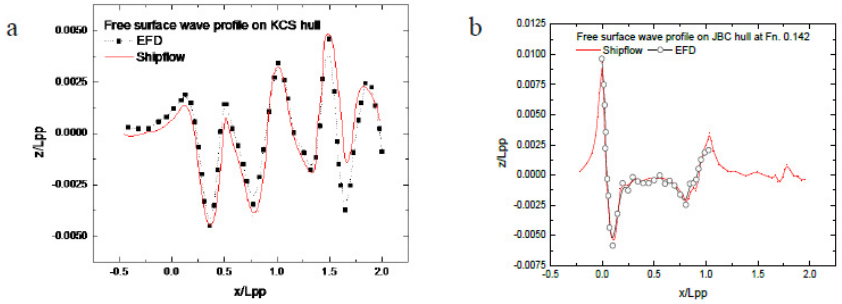

Fig. 7: Free-surface wave profile around (a) KCS ; (b) JBC hull

4.3. Verification and validation (V&V) study for bare hull resistance

A Verification and Validation (V&V) study for total resistance coefficients of both hull has been done according to the ITTC recommended procedures [9] based on numerical and modeling uncertainty respectively. Verification is done for three different grid densities from fine (S_1) to coarse (S_3) as shown in Table 2, 3. Fig. 8 shows numerical and data uncertainty for KCS and JBC hull with EFD [10] results.

Table 2: V&V study for KCS bare hull resistance prediction, $Re = 1.26 \times 10^7$, $Fr = 0.260$

		V&V Study					
Parameters		**EFD (D)**	**Grid#3 (S_3)**	**Grid#2 (S_2)**	**Grid#1 (S_1)**	**U_D %S_1**	**U_{SN} %**
$C_t \times 10^3$	Value	3.711	3.968	3.763	3.738	1.0	0.715
	E%D		-6.925	-1.401	-0.728		
$C_w \times 10^3$	Value		1.6172	1.4962	1.4952		
$C_v \times 10^3$	Value		2.3508	2.2668	2.2428		

4.4. Propeller open water characteristics

Propeller open water characteristics are investigated by applying Open Water (POW) simulations of Shipflow for various advance ratios which proves fairly good agreement with EFD [10] as shown in Fig. 9.

4.5. Self propulsion characteristics at varying longitudinal rudder positions

Definition sketch of longitudinal distance of rudder (b) to propeller diameter (D) is shown in Fig. 10.

Table 3: V&V study for KCS bare hull resistance prediction, $Re = 7.46 \times 10^6$, $Fr = 0.142$

		V&V Study					
Parameters		**EFD (D)**	**Grid#3 (S_3)**	**Grid#2 (S_2)**	**Grid#1 (S_1)**	**U_D %S_1**	**U_{SN} %**
$C_t \times 10^3$	Value	4.289	4.175	4.196	4.22	1.0	0.825
	E%D		2.658	2.168	1.61		
$C_w \times 10^3$	Value		0.313	0.3318	0.3318		
$C_v \times 10^3$	Value		3.862	3.864	3.868		

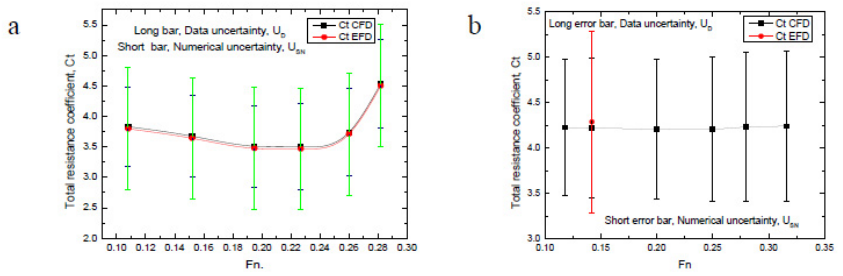

Fig. 8: Verification and Validation for resistance coefficients (a) KCS ; (b) JBC

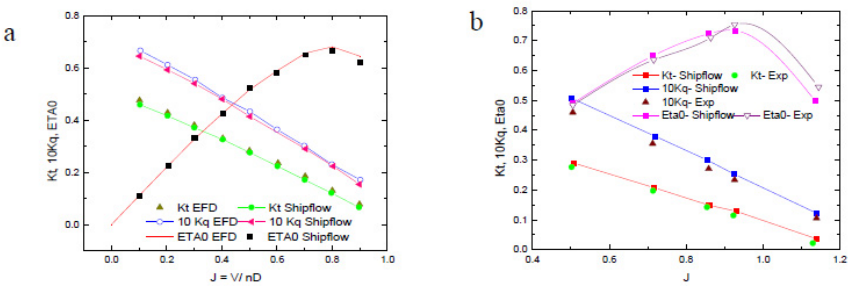

Fig. 9: Comparison of open water hydrodynamic characteristics of (a) KP505 and ; (b) DTMB 4119 propeller CFD and EFD results

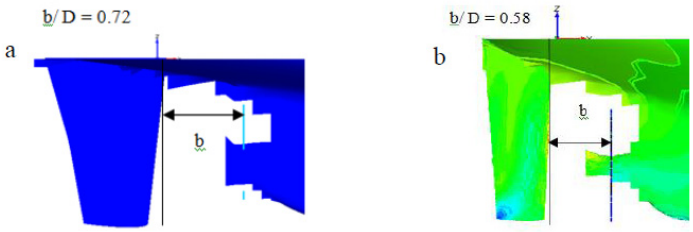

Fig. 10: Definition sketch for longitudinal distance of rudder to propeller diameter (b/D) (a) KCS hull ; (b) JBC hull

Table 4 shows self-propulsion characteristics for five and six different longitudinal positions of rudder for KCS and JBC respectively. Maximum thrust is developed by the propeller of the ship at extreme rudder position, $b/D = 0.804$ for KCS hull with 29.17 knot speed and at $b/D = 0.58$ for JBC hull with 14.47 knot speed.

Table 4: Comparison between zonal and global approach

KCS					JBC				
b/D	**Ship res.,R_S [kN]**	**Thrust, T_S [kN]**	**Torque, Q_S [kN.m]**	**Deliv. Power, P_D [MW]**	**b/D**	**Ship res.,R_S [kN]**	**Thrust, T_S [kN]**	**Torque, Q_S [kN.m]**	**Deliv. Power, P_D [MW]**
0.804	4284.304	4179.63	1151	13.647	0.58	2078.161	1533.29	559	3.396
0.72	4342.297	4156.13	1170	14.011	0.53	2078.054	1516.28	558	3.385
0.63	4319.141	4159.70	1164	13.883	0.50	2094.093	1512.22	565	3.449
0.54	4333.702	4154.30	1168	13.969	0.44	2103.362	1480.86	579	3.565
0.37	4344.245	4147.98	1168	13.976	0.40	2097.940	1506.78	576	3.590
					0.35	2093.155	1449.33	587	3.601

4.6. *Wake fraction and Axial velocity contour at stern*

Propeller wake fraction at propeller disc at optimum rudder positions are shown in Fig.11 from which it is apparent that maximum wake fraction occurs at the points where the propeller disc is near to the hull. Axial velocity contour around the stern region of the KCS and JBC hulls at stern positions of $x = 0.95$ are shown in Fig.12. It shows good agreement with the experimental results [10] for both hull.

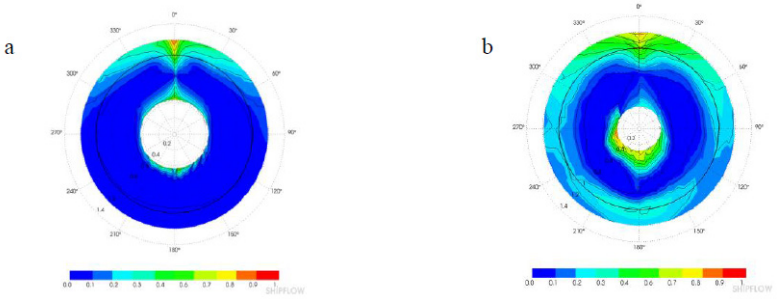

Fig. 11: Wake fraction at propeller disc (a) KCS hull at $b/D = 0.72$; (b) JBC hull $b/D = 0.35$

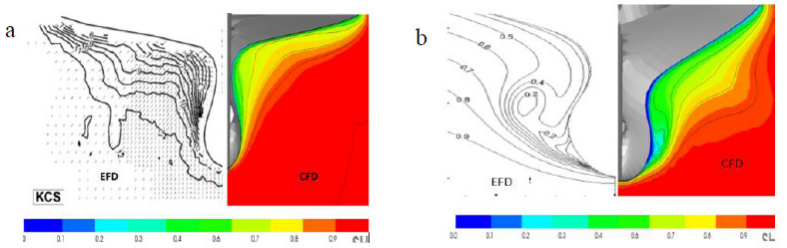

Fig. 12: Axial velocity contour at stern (a) KCS hull at $b/D = 0.72$; (b) JBC hull $b/D = 0.35$ both at $x = 0.95$

4.7. *Efficiency of zonal approach over global approach*

Bare ship hull resistance is computed first with zonal approach and compared with global approach. It has been found that the former complete the whole analysis in far more less time than the latter approach for very coarse

and coarse mesh size. Furthermore, with zonal approach results have been obtained for both hull with medium and fine mesh sizes whereas, global approach is incapable of dealing with the similar mesh size as shown in Table 5. Consequently, it is also failed to compute self propulsion characteristics.

Table 5: Comparison between zonal and global approach

	KCS		JBC	
	Zonal	**Global**	**Zonal**	**Global**
Mesh Size (Million, M)	**Time (min)**	**Time (min)**	**Time (min)**	**Time (min)**
Very Coarse (0.213 M)	18	145	18	157
Coarse (0.446 M)	30	230	33	243
Medium (0.744 M)	53	—	57	—
Fine (1.218 M)	77	—	83	—

5. Conclusions

In this paper, flow field around modern benchmark ship hull are determined including self propulsion characteristics at varying rudder positions. From the above mentioned results and discussions, following conclusions can be drawn:

i Zonal approach for computing flow characteristics is more effective than global approach in regard to both time and expense.
ii Various hydrodynamic characteristics of ships and propellers show good agreement with available experimental results.
iii Lifting line method coupled with RANS solver can be used effectively to determine self propulsion characteristics of marine propellers at changing rudder positions. The effect of rudder decreases with the increase in distance of rudder position from the propeller.

References

[1] L.O. Lübke, Numerical simulation of the flow around the propelled KCS, CFD Workshop Tokyo, Tokyo, Japan, 2005.
[2] T. Hino, CFD-based estimation of propulsive performance in ship design, Proc. 26th Symp Naval Hydrodynamics, Rome, Italy, 2006.
[3] J. Kim, K.S. Kim, G.D. Kim, I.R. Park and S.H. Van, Hybrid RANS and potential based numerical simulation for self-propulsion performances of the practical container ship, J. Ship Ocean Tech., 10 (2006) 1-11.
[4] Y. Tahara, R.V. Wilson, P.M. Carrica and F. Stern, RANS Simulation of a Container Ship Using a Single-Phase Level Set Method with Overset Grids and Prognosis for Extension to Self-Propulsion Simulator, J. Mar. Sci. Technol., 11 (2006) 209-228.
[5] J.E. Choi, K.S. Min, J.H. Kim and H.W. Seo, Resistance and Propulsion Characteristics of Various Commercial Ships Based on CFD results, Ocean Eng., 37 (2010) 549-566.
[6] Huiping Fu, Thad J. Michael and Pablo M. Carrica, A method to perform self-propulsion computations with a simplified body-force propeller model, Proc. Twenty-fifth International Ocean and Polar Engineering Conference., Hawaii, USA, 2015.
[7] W. J. Kim, S. H. Van. D. H. Kim, Measurement of flows around modern commercial models, Experiments in fluids 31(2001), Springer Verlag, 567-578.
[8] N. Sakamoto and K. Kume, Numerical towing tank procedure for JBC in self-propulsion with rotating propeller and energy saving duct, in JASNAOE Spring Annual Meeting, Fukuoka, Japan, 2016.
[9] ITTC Recommended procedures and guidelines 7.5-03-02-01, Uncertainty analysis in CFD examples for resistance and flow, 1999.
[10] Tokyo 2015: A Workshop on CFD in Ship Hydrodynamics, Tokyo, Japan, 2015.